MEaSUREs ITS_LIVE Regional Glacier and Ice Sheet Surface Velocities, Version 1

USER GUIDE

How to Cite These Data

As a condition of using these data, you must include a citation:

Gardner, A., M. Fahnestock, and T. Scambos, 2022. *MEaSUREs ITS_LIVE Regional Glacier and Ice Sheet Surface Velocities, Version 1*. [Indicate subset used]. Boulder, Colorado USA. NASA National Snow and Ice Data Center Distributed Active Archive Center. https://doi.org/10.5067/6II6VW8LLWJ7.

We also request that you acknowledge the author(s) of this data set by referencing the following peer reviewed publication:

Gardner, A. S., G. Moholdt, T. Scambos, M. Fahnstock, S. Ligtenberg, M. van den Broeke, and J. Nilsson. 2018. Increased West Antarctic and unchanged East Antarctic ice discharge over the last 7 years, *The Cryosphere*, 12(2):521–547. https://doi.org/10.5194/tc-12-521-2018.

FOR QUESTIONS ABOUT THESE DATA, CONTACT NSIDC@NSIDC.ORG

FOR CURRENT INFORMATION, VISIT https://nsidc.org/data/NSIDC-0776

National Snow and Ice Data Center

TABLE OF CONTENTS

DATA DESCRIPTION

The Inter-Mission Time Series of Land Ice Velocity and Elevation (ITS_LIVE) project, part of NASA's Making Earth System Data Records for Use in Research Environments (MEaSUREs) 2017 program, was created to provide global, low-latency and, high temporal resolution measurements of glacier and ice sheet surface velocities and elevation changes.

This data set consists of annual mean surface velocities compiled for select glacier-covered regions spanning 1985 to 2018 (subject to image availability and quality). Velocities were derived by applying the autonomous Repeat Image Feature Tracking algorithm (autoRIFT) processing chain (Gardner et al., 2018; Lei et al., 2021) to imagery from Landsat 4, 5, 7, and 8. Data scarcity and/or low radiometric quality (e.g., band saturation) are significant limiting factors for many regions during the earlier years of the data record. Annual, global coverage is nearly complete after the 2013 launch of Landsat 8.

Parameters

Ice velocity (x and y components and velocity magnitude)

File Information

Format

Data are provided as NetCDF-4 (.nc) files.

File Contents

Each NetCDF file contains the parameters listed in Table 1, gridded at 240 m or 120 m over the regional map areas. Figure 1 shows an example of Antarctic velocities at 240 m resolution for the years 1990, 2008, and 2018.

Table 1. Parameter Names and Descriptions

Parameter Name	Description	Units	Class
x	Map projected x coordinate	m	double
y	Map projected y coordinate	m	double
vx	Velocity component in x direction	m/yr	short
vy	Velocity component in y direction	m/yr	short
v	Velocity magnitude	m/yr	short

Parameter Name	Description	Units	Class
vx_err	Error in v_x	m/yr	float
vy_err	Error in v_y	m/yr	float
v_err	Error in v	m/yr	float
date	Effective date (error-weighted, average center date for the pixel)	days since 01 January 0000*	float
dt	Effective date separation (average number of days between image pairs). dt > 300 days can be considered average annual velocities, while dt < 180 represent average summer values.	days	float
count	Number of velocities used in weighted average	count	ushort
mapping	Projected coordinate system details (NSIDC Sea Ice Polar Stereographic North)	N/A	float
chip_size_max	Maximum accepted search chip size	m	ushort
ocean	Ocean mask	binary	ubyte
rock	Rock mask	binary	ubyte
ice	Ice mask	binary	ubyte

*The date is stored as a serial date number that represents the whole number of days from a fixed, preset date (January 0, 0000) in the proleptic ISO calendar. E.g., 1 January 2000 = 730486 days from January 0, 0000.

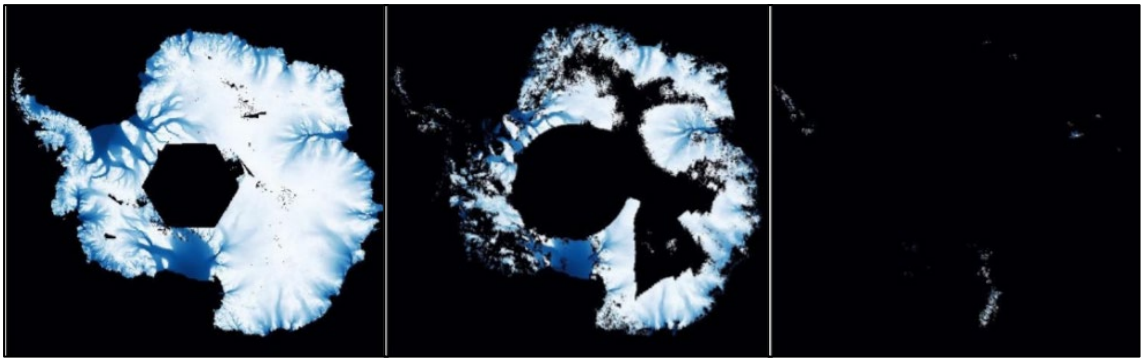

Figure 1. Antarctic velocities for the years 2018 (left), 2008 (center), and 1990 (right).

Naming Convention

Example File Name

ALA_G0240_2018.nc

Naming Convention

[RRR]_G[XXXX]_[YYYY].ext

File names specify the region (see Figure 2), spatial resolution, and year using the variable described in the following table:

Table 2. File Name Variables and Descriptions

Variable	Description
RRR	Region ID: ALA = Alaska and Western North America ANT = Antarctica CAN = Arctic Canada GRE = Greenland HMA = High Mountain Asia ICE = Iceland PAT = Patagonian icefields SRA = Svalbard and the Russian Arctic
GXXXX	Resolution (m), preceded by "G". Values are either G0240 (240 m) or G0120 (120 m)*.
YYYY	Four-digit year of survey. A value of 0000 denotes a time-averaged or static velocity (i.e., the error-weighted average of all years of data).
.ext	.nc (NetCDF)

*Only ALA, SRA, and time-averaged velocity data (denoted by YYYY = 0000) are available at 120 m resolution

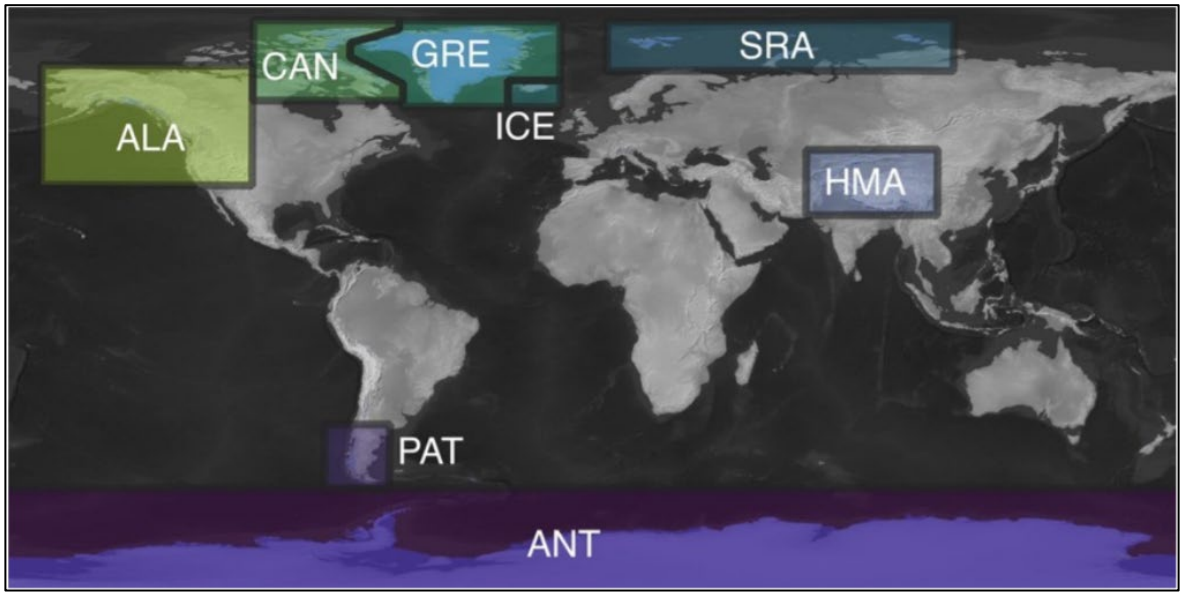

Figure 2. Approximate Geographical Locations of the Eight Mapped Regions

Spatial Information

Coverage

The spatial coverage encompasses the eight regions listed in Table 3.

Table 3. Spatial Coverage By Region

Region	Coverage (°)
ALA (Alaska and Western North America)	N: 62.23 S: 47.23 E: -107.65 W: -159.45
ANT (Antarctica)	N: -57.62 S: -90 E: 127.41 W: -128.81
CAN (Arctic Canada)	N: 84.09 S: 61.62 E: -50.14 W: -109.69
GRE (Greenland)	N: 81.62 S: 58.67 E: 8.23 W: -90.17
HMA (High Mountain Asia)	N: 45.93 S: 24.64 E: 104.29 W: 65.36
ICE (Iceland)	N: 67.18 S: 62.91 E: -13.41 W: -24.54
PAT (Patagonian icefields)	N: -45.66 S: -55.41 E: -68.55 W: -74.52
SRA (Svalbard and Russian Arctic)	N: 45.93 S: 24.64 E: 104.29 W: 65.36

Resolution

240 m x 240 m (all regions)

120 m x 120 m (ALA, SRA, plus time-averaged velocity mosaics* denoted by “0000” in file name)

*Cubic spline interpolation of underlying 240 m data.

Geolocation

Table 4 contains information to geolocate the 240 m × 240 m grids in each of the eight regions.

Table 4. Region and Geolocation Information

Region	EPSG code	X_{min}	X_{max}	Y_{min}	Y_{max}
ALA	3413	-4632847.5	-2791807.5	-1443712.5	1269007.5
ANT	3031	-2678287.5	2816512.5	-2154112.5	2259727.5
CAN	3413	-12382877.5	-259327.5	-2881792.5	-585712.5
GRE	3413	-645007.5	858112.5	-3369472.5	-641392.5
HMA	102027	-2159887.5	652672.5	-264832.5	1643407.5
ICE	3413	981232.5	1416832.5	-2630272.5	-2304112.5
PAT	32718	537712.5	909952.5	3859327.5	4930447.5
SRA	3413	591472.5	1850752.5	-712192.5	1092367.5

Temporal Information

Coverage

1985 to 2018

Resolution

Annual

DATA ACQUISITION AND PROCESSING

Acquisition

This data set utilizes imagery from the following sources:

- Landsat 4 Thematic Mapper, Band 2 (1982 to 1993)
- Landsat 5 Thematic Mapper, Band 2 (1984 to 2013)
- Landsat 7 Enhanced Thematic Mapper Plus, Band 8 (1999 to 2018)
- Landsat 8 Operational Land Imager, Band 8 (2013 to 2018)

All images with cloud cover ≤ 60% (per the image metadata) were processed. Landsat imagery is provided courtesy of the USGS and was downloaded from Google Cloud (https://cloud.google.com/storage/docs/public-datasets/landsat).

Processing Steps

Image Preprocessing

All images were preprocessed using a 5 × 5 Wallis operator to normalize for local variability in image radiance due to shadows, topography, and sun angle, which can produce artifacts in surface flow derived from feature tracking. For Landsat 4 and 5, Fourier filtering was used to remove along-track artifacts introduced by the Thematic Mapper whisk broom sensor. Missing Landsat 7 images, due to the Scan Line Corrector failure (SLC-off) in May of 2003, were filled with random noise to prevent them from contributing to the correlation peak amplitude used by the feature tracking.

Image-pair velocities (auto-RIFT v1)

This data set is generated by using Version 1 of autoRIFT (Gardner et al., 2018) to identify surface displacements in image pairs from repeat orbits and adjacent or near-adjacent orbits lying within a specified distance. Furthermore, image pairs were only collected from the same satellite position ("same-path-row") when separated in time by fewer than 546 days. This approach was used for all satellites in the Landsat series (L4 to L8).

To increase data density prior to the launch of Landsat 8, images acquired from differing satellite positions—generally in adjacent or near-adjacent orbit swaths (i.e., "cross-path-row")—are also processed if they have a time separation between 10 and 96 days and an acquisition date prior to when operational Landsat 8 data began on 14 June 2013.

Feature tracking of cross-path-row image pairs produces velocity fields with a lower signal-to-noise ratio due to residual parallax from imperfect terrain correction. Matching features in pre-processed, same-path-row and cross-path-row image pairs were identified by using a Gaussian kernel to oversample the correlation surface by a factor of 16 and find local, normalized cross-correlation (NCC) maxima at sub-pixel resolutions.

A sparse grid, pixel-integer NCC search (1/16 of the density of full search grid) was used to determine areas of coherent correlation between image pairs (see the Normalized Displacement Coherence filter described in Gardner et al., 2018). Results from the sparse search were then used

to guide a dense search, which spaces search centers such that no overlap exists between adjacent template windows. Areas of unsuccessful retrievals, as determined by the NDC filter, were searched with progressively increasing template chip sizes. Minimum and maximum acceptable template chip sizes for each search center were defined geographically depending on land surface type (ice or rock); spatial gradient of a reference velocity mapping; distance from the ocean; and distance from an ice edge. The data were then filtered one last time using the NDC filter, followed by a light interpolation to fill in small data gaps. The location of interpolated values are recorded in interp_mask with a value of "1".

To reduce computational demand, autoRIFT employs a downstream search that centers the NCC search template window in the search image at the downstream location of the expected displacement between the two image pairs, as determined from the reference velocity. The NCC search radius is unique in both the x and y directions and varies spatially. It is defined according to the surface type (ice or rock), magnitude of the component reference velocity (v_x, v_y), and the distance from the ocean. Ocean area is identified according to the Global Self-consistent, Hierarchical, High- resolution Geography Database (GSHHG).

Land ice in Greenland was identified using a data set provided by F. Paul (Bolch et al., 2013); Antarctica land ice was identified using Depoorter et al. (2013). Everywhere else, land ice is determined using the Randolf Glacier Index release 3.2 (see https://www.glims.org/RGI/). Rock is defined as neither ocean nor land ice.

Annual Velocity Maps

Annual velocity maps are created by taking the error-weighted average of all image pair velocity fields having a center-date that falls within that calendar year. The weight of each image-pair velocity field is calculated as:

$$w_{x/y,i} = \frac{1}{\sigma_{x/y,i^2}},$$

where *x/y* denotes the velocity component of each image pair velocity *i*. This is done iteratively to co-register image pair velocities that do not intersect the "stable" reference surface and, therefore, do not have geolocation offset corrections. In the iterative process, all image-pair velocities with geolocation offset corrections are combined to create an annual velocity field that is then used to co-register image pair velocities that lack geolocation offset corrections. This secondary co-registration ties unregistered pairs to the annual velocity field where the error in the annual velocity field is less than 50 m/yr. It is typically only utilized for large Antarctic ice shelves where the distances to exposed rock and/or slow-moving ice (less than 15 m/yr) can be large.

More information is available in the MEaSUREs ITS_LIVE Regional Glacier and Ice Sheet Surface Velocities product description document.

Quality, Errors, and Limitations

Image geometry between same-path-row image pairs is highly stable; however, geolocation errors of up to 15 m can exist in the x and y coordinate. If uncorrected, a geolocation error of, say, $\sqrt{15^2 + 15^2}$ = 21 m between two images separated in time by 16 days would introduce a bias in velocity of as much as 480 m/yr. To correct for these errors, the component velocities v_x and v_y are tied to a "stable" surface—the median of each velocity component is set to zero over rock surfaces and set to the median reference velocity over slow-moving areas (ice movement of <15 m/yr) of Greenland and Antarctica. For Greenland, the MEaSUREs Greenland Annual Ice Sheet Velocity Mosaics from SAR and Landsat, Version 1 data are used as the reference velocity; for Antarctica, the MEaSUREs InSAR-Based Antarctica Ice Velocity Map, Version 2 data are used.

The uncertainty of each image pair velocity field is set equal to the standard deviation in component velocities measured over a stable surface after applying the geolocation offset correction (if available). If an image pair velocity field does not intersect a stable surface, the errors in v_x and v_y (parameters vx_err and vy_err) are set to the root sum of squares (RSS) of the pointing uncertainty of both images. If the image pair velocity is successfully co-registered during the creation of the annual mosaic (see below), this error is updated to the standard deviation of the difference between the image pair component velocities and the annual mean component velocities.

Velocities are calculated from imagery that has been map projected. This can introduce scale errors of up to a few percent that are dependent on the projection used and the location of the imagery. This distortion is corrected for such that derived velocities represent horizontal velocities that would be measured by an observer on the ground. This has several implications:

1. When using ITS_LIVE image pair velocities to calculate glacier flux, the flux-gate cross-section needs to be corrected for projection scale distortion (the image pair velocities do not need to be corrected).
2. When calculating Lagrangian paths in map coordinates, image pair velocities should be scaled from velocities in ground units to velocities in map units, to produce the appropriate speed in map coordinates.

Annual Mosaics (auto-RIFT v1)

Image-pair velocity fields can be contaminated by match blunders, such as matching along shadow edges or when surfaces are obscured by clouds in one of the two images. Component velocities that deviate by more than three times the interquartile range, from the median of all co-located

pixels, are assumed to be gross outliers and removed. For normally distributed data, this approximates a 5σ filter.

The error of the final annual mosaic is taken as:

$$\sigma_{x/y} = \sqrt{\frac{1}{\sum 1/\sigma_{x/y,i}^2}} = \sqrt{\frac{1}{\sum w_{x/y,i}}}$$

This approach, while allowing for the formal propagation of errors, typically produces errors that are unrealistically low. As such, the data providers suggest that the provided errors (vx_err, vy_err, and v_err), along with image-pair count (count), should be used as qualitative metrics for assessing errors.

Annual mosaics are also provided with an effective date and image-pair time separation, estimated for each pixel as a weighted average of the individual pairs' dates and time spans. A best estimate of the mean (or static) flow field for each region is provided by taking the weighted average of all years of data.

SOFTWARE AND TOOLS

NetCDF files can be accessed using geospatial software, including free and open source packages such as QGIS and Panoply.

VERSION HISTORY

Version 1 (August 2022)

RELATED DATA SETS

- Global Land Ice Velocity Extraction from Landsat 8 (GoLIVE), Version 1
- Landsat 8 Ice Speed of Antarctica (LISA), Version 1
- MEaSUREs Greenland Ice Velocity: Selected Glacier Site Velocity Maps from InSAR, Version 1
- MEaSUREs Annual Antarctic Ice Velocity Maps 2005-2017, Version 1

RELATED WEBSITES

- ITS_LIVE project
- GrIMP Data at NSIDC
- Antarctic Ice Sheet Velocity and Mapping Project (AIV)

CONTACTS AND ACKNOWLEDGMENTS

Alex Gardner
Jet Propulsion Laboratory
California Institute of Technology
Pasadena, CA 91109

Mark Fahnestock
Geophysical Institute
University of Alaska Fairbanks
Fairbanks, AK 99775

Ted Scambos
Earth Science & Observation Center
Cooperative Institute for Research in Environmental Sciences
University of Colorado Boulder
Boulder, CO 80309

REFERENCES

T. Bolch, L. Sandberg Sørensen, S. B. Simonsen, N. Mölg, H. Machguth, P. Rastner, F. Paul. 2013. Mass loss of Greenland's glaciers and ice caps 2003-2008 revealed from ICESat laser altimetry data. *Geophysical Research Letters*, 40(5), 875–881. https://doi.org/10.1002/grl.50270

Depoorter, M. A., J. L. Bamber, J. A. Griggs, J. T. M. Lenaerts, S. R. M. Ligtenberg, M. R. van den Broeke, and G. Moholdt. 2013. Calving fluxes and basal melt rates of Antarctic ice shelves. *Nature*, 502(7469), 89–92. https://doi.org/10.1038/nature12567

Gardner, A. S., G. Moholdt, T. Scambos, M. Fahnestock, S. Ligtenberg, M. van den Broeke, and J. Nilsson. 2018. Increased West Antarctic and unchanged East Antarctic ice discharge over the last 7 years. *The Cryosphere*, 12(2), 521–547. https://doi.org/10.5194/tc-12-521-2018

Joughin, I., B. E. Smith, I. M. Howat, T. Scambos, and T. Moon. 2010. Greenland flow variability from ice-sheet-wide velocity mapping. *Journal of Glaciology*, 56(197), 415–430. https://doi.org/10.3189/002214310792447734

Lei, Y., A. Gardner, and P. Agram. 2021. Autonomous repeat image feature tracking (autoRIFT) and its application for tracking ice displacement. *Remote Sensing*, 13(4):749. https://doi.org/10.3390/rs13040749

Mouginot, J., B. Scheuchl, and E. Rignot. 2012. Mapping of Ice Motion in Antarctica Using Synthetic-Aperture Radar Data. *Remote Sensing*, 4(9), 2753–2767. https://doi.org/10.3390/rs4092753

Rignot, E., J. Mouginot, and B. Scheuchl. 2011. Ice Flow of the Antarctic Ice Sheet. *Science*, 333(6048), 1427–1430. https://doi.org/10.1126/science.1208336

DOCUMENT INFORMATION

Publication Date

August 2022

Date Last Updated

September 2022